The role of organic condensation on ultrafine particle growth during nucleation events

D. Patoulias[1,2], C. Fountoukis[2], I. Riipinen[3] and S. N. Pandis[1,2,4]

[1] Department of Chemical Engineering, University of Patras, Patras, Greece

[2] Institute of Chemical Engineering Sciences, Foundation for Research and Technology Hellas (FORTH/ICE-HT), Patras, Greece

[3] Department of Applied Environmental Science & Bert Bolin Centre for Climate Research, Stockholm University, Stockholm, Sweden

[4] Department of Chemical Engineering, Carnegie Mellon University, Pittsburgh, PA 15213, USA

Abstract

A new aerosol dynamics model (DMANx) has been developed that simulates aerosol size/composition distribution and includes the condensation of organic vapors on nanoparticles through the implementation of the recently developed Volatility Basis Set framework. Simulations were performed for Hyytiala (Finland) and Finokalia (Greece), two locations with different organic sources where detailed measurements were available to constrain the new model. We investigate the effect of condensation of organics and chemical aging reactions of secondary organic aerosol (OA) precursors on ultrafine particle growth and particle number concentration during a typical springtime nucleation event in both locations. This work highlights the importance of the pathways of oxidation of biogenic volatile organic compounds and the production of extremely low-volatility organics. At Hyytiala, organic condensation dominates the growth process of new particles. The low-volatility secondary OA contributes to particle growth during the early growth stage, but after a few hours most of the growth is due to semi-volatile secondary OA. At Finokalia, simulations show that organics have a complementary role to new particle growth contributing 45% to the total mass of new particles. Condensation of organics increases the number concentration of particles that can act as CCN (N_{100}) by 13% at Finokalia and 25% at Hyytiala during a typical spring day with nucleation. The sensitivity of our results to the surface tension used is discussed.

1. Introduction

New particles are introduced in the atmosphere by i) direct emissions from a variety of (primary) sources and, ii) nucleation (in situ formation). Nucleation and subsequent growth of new particles is often observed in most areas of the globe (Kulmala et al., 2004) and represents an important source of ambient aerosol number concentration. Fresh particles formed by nucleation can either grow through condensation of vapors (e.g. sulfuric acid and ammonia, organics) to larger sizes or can be lost by coagulation with pre-existing larger particles. The newly formed particles that manage to survive coagulation can grow to larger sizes and become cloud condensation nuclei (CCN) affecting the cloud droplet number concentration (Adams and Seinfeld, 2002). Nucleation and subsequent growth by condensation can be an important source of CCN (Lihavainen et al., 2003; Kerminen et al., 2005; Laaksonen et al., 2005; Merikanto et al., 2009; Makkonen et al., 2009; Pierce and Adams, 2009b; Wang and Penner, 2009; Yu and Luo, 2009; Spracklen et al., 2010). Changes in CCN concentration affect cloud optical properties and cloud lifetime, perturbing the energy balance of the planet (Twomey 1974; 1977; 1991; Albrecht, 1989). An increase of the number concentration of particles that can act as CCN results in higher cloud droplet number concentrations and brighter clouds with longer lifetimes. Measurements of CCN at a non-urban site in Germany suggested that CCN concentrations are mainly determined by the aerosol number size distribution while the composition of aerosol plays a secondary role (Dusek et al., 2006). Furthermore, nanoparticles can affect human health by deposition in the human lungs or the neurological system. For small particles the damage can be greater due to the larger surface area per unit mass (Peters et al., 1997; Donaldson et al, 1998; 2002). The effects of aerosol composition on human health are still uncertain (Godleski et al., 2000).

Several mechanisms have been proposed to explain in-situ particle formation. These include sulfuric acid–water binary nucleation (Nilsson and Kulmala, 1998; Vehkamaki et al., 2002), ternary nucleation (Coffman and Hegg, 1995; Korhonen et al., 1999; Kulmala et al., 2002; Napari et al., 2002), nucleation of organic vapors (Marti et al., 1997; Zhang et al., 2004), ion-induced nucleation (Laakso et al., 2002) and halogen-oxide nucleation (Hoffmann et al., 2001). The binary nucleation mechanism has been the most commonly used in atmospheric models with the critical cluster assumed to be composed of H_2SO_4 and H_2O. Ternary nucleation theory usually includes ammonia (NH_3) as a third component. It is possible that other compounds (e.g. organics, amines) may play a similar role under certain conditions (Bonn et al., 2008; Kurten et

al., 2008; Metzger et al., 2010; Smith et al., 2010; Berndt et al., 2010; Zhao et al., 2011; Kirkby et al., 2011; Almeida et al., 2013; Riccobono et al., 2014). A strong correlation has been found between measured aerosol nucleation rate and the gas-phase sulfuric acid concentration (Weber et al., 1996; Sihto et al., 2006; Riipinen et al., 2007; Kuang et al., 2008; Nieminen et al., 2009; Paasonen et al., 2009; 2010) in various sites in Europe and the United States. Nucleation events observed in sulfur-rich regions like the northeastern US appear to be initiated by the formation of gas-phase H_2SO_4 (via SO_2 oxidation) but terminated by the exhaustion of gas-phase NH_3 or other bases (Jung et al., 2008). Ambient measurements and some laboratory studies (Sipila et al., 2010) have revealed a linear or squared correlation between new particle formation rate and concentration of sulfuric acid.

Significant uncertainties arise also from the incomplete understanding of the identity of the species involved in the growth of these nuclei (Kulmala et al., 2004). Field measurements (Eisele and McMurry, 1997; Weber et al., 1998, 1999; Janson et al., 2001) and model simulations (Kerminen et al., 2001; Kulmala et al., 2000; Pirjola and Kulmala, 2001; Anttila and Kerminen, 2003) indicated that the condensation of sulfuric acid alone is often not sufficient to explain the observed growth rates of fresh particles (Riipenen et al., 2011). The growth of fresh nuclei could be due to the condensation of organic species (Kerminen et al., 2000; Anttila and Kerminen, 2003), heterogeneous reactions (Zhang and Wexler, 2002), or ion-enhanced condensation (Laakso et al., 2002).

Jung et al. (2010) developed a three-dimensional regional chemical transport model (CTM), PMCAMx-UF, with detailed aerosol microphysics (Gaydos et al., 2007; Karydis et al., 2007) that has been used for simulations over the US and Europe (Fountoukis et al., 2012). In Europe the model predictions were compared against size distribution measurements from seven sites (Fountoukis et al., 2012). The model was found to reproduce more than 70% of the hourly number concentrations of particles larger than 10 nm (N_{10}) within a factor of 2. For particles larger than 100 nm (N_{100}, a proxy for the number of particles that can act as CCN) a systematic underprediction was seen. The growth rates were also underpredicted (with smaller errors in sites where the sulfate to organics mass ratio is high (e.g., Melpitz)) possibly because of insufficient organic vapor condensation (Fountoukis et al., 2012) as the model did not explicitly include secondary organic aerosol (SOA) condensation on ultrafine particles. Yu (2011) and Riipinen et al. (2011) studied the condensation of organics on ultrafine particles using global CTMs. Yu

(2011) estimated that the concentration of low volatility organics is a factor of 2-20 higher than the H_2SO_4 concentration in many continental locations and can significantly enhance the growth rate of freshly nucleated particles. He compared predicted particle size distributions with field measurements in a boreal forest site (Hyytiala, Finland) showing that the condensation of low volatility organics can bring the simulation results closer to the observations. Riipinen et al. (2011) estimated that roughly half of the condensed organic mass needs to be distributed proportionally to the aerosol surface area to explain the observed aerosol growth. These organic compounds need to have both high yields and very low volatility which is inconsistent with laboratory observations of the first generation yields of SOA from biogenic precursors (Presto et al., 2006, Pathak et al., 2007, Pandis et al., 2013). Pierce et al. (2011) estimated that the average effective saturation concentration (C^*) of condensing organics needs to be 10^{-3}–10^{-2} μg m^{-3} or less to enhance the growth of freshly nucleated particles.

Secondary organic aerosol accounts for a significant mass fraction (20-90%) of sub-micrometer particulate matter at many locations around the globe and is one of the most dominant particle components in the atmosphere (Jimenez et al., 2009). The sources and the chemical composition of OA are still uncertain due to the large number (tens of thousands) of different atmospheric organic compounds (Goldstein and Galbally, 2007). OA has been the subject of numerous studies during the last decade (Hallquist et al., 2009) but remains the least understood component of atmospheric aerosols. The organic aerosol composition continuously evolves with time due to various chemical reactions (Kanakidou et al., 2005). Gas-phase oxidation of volatile organic compounds (VOCs) produces semi-volatile products that can then condense to the particulate phase. Products with high vapour pressures can be oxidized to species with lower vapour pressures that can then condense on preexisting particles. The chemical aging (further oxidation) of semivolatile organic compounds is an important source of OA mass (Donahue et al., 2006). Until recently most CTMs described secondary OA formation using two surrogate species per VOC (Odum et al., 1996). This approach is computationally expensive due to the large number of products while the use of only two products per VOC limits the concentration range and the accuracy of this approach (Murphy et al., 2009). SOA vapors may undergo further gas-phase oxidation and simulation of this aging process would require introduction of even more species (Ng et al., 2006). The Volatility Basis Set (VBS) framework (Donahue et al., 2006) was proposed to address these problems, describing the complete

volatility range of OA compounds using logarithmically spaced bins characterized by an effective saturation concentration, C^* (in μg m^{-3}). This framework has been shown to work well for simulations of aerosol mass distributions in 3-D CTMs (Murphy et al., 2009; Tsimpidi et al., 2010; Fountoukis et al., 2011).

The overall objective of this work is to examine the contribution of organic vapor condensation to the growth of fresh particles formed by nucleation and whether this condensation can explain the observed growth rate of new particles. We extend the Dynamic Model for Aerosol Nucleation (DMAN) of Jung et al. (2006) which originally assumed that particles can grow only by condensation (of sulfuric acid and ammonia) and coagulation. In this work, we develop an updated version of DMAN (DMANx) which includes the condensation of organic vapors on particles and the most recent version of the VBS framework. We estimate for the first time the effect of the chemical aging gas-phase reactions of SOA components on ultrafine particle growth. We examine the effects of condensation of organics, the gas-phase chemical aging reactions, and the Kelvin effect on the predicted particle number concentrations. We focus on the composition of fresh particles during nucleation events as well as during their subsequent growth, in two remote continental locations, Hyytiala, Finland and Finokalia, Greece where there are sufficient measurements available to constrain the new model. This is the first step towards improving the predictions of the 3-D CTM, PMCAMx-UF.

2. Model description

DMAN simulates nucleation, coagulation and condensation/evaporation for a multi-component atmospheric aerosol (Jung at el., 2006). It uses the Two-Moment Aerosol Sectional (TOMAS) algorithm of Adams and Seinfeld (2002) which is based on the sectional approach for the description of the aerosol size composition distribution. TOMAS is an adaptation of cloud microphysics algorithms (Tzivion et al., 1987; 1989) to aerosol processes, is computationally efficient, and tracks both mass and number concentrations simultaneously. The aerosol size distribution is described with 41 size sections with the lowest size bin corresponding to a 3.75×10^{-25} kg dry aerosol mass per particle. That corresponds to 0.8 nm dry diameter assuming a density of 1.4 g cm^{-3}. Each successive section has double the mass of the previous one. The largest bin corresponds to a diameter of 10 μm.

2.1 Nucleation

DMAN has the option of using a number of nucleation parameterizations. In this work, the rate of nucleation is calculated using a scaled ternary nucleation parameterization based on the original expressions of Napari et al. (2002) if the NH_3 concentration exceeds 0.01 ppt, and the binary parameterization of Vehkamaki et al. (2002) if it is less than this threshold value. The original NH_3-H_2SO_4-H_2O parameterization has been successful in predicting the presence or lack of nucleation events (Gaydos et al., 2005) in sulfur rich environments. However, it overpredicts ultrafine number concentrations during nucleation events (Gaydos et al., 2005; Yu, 2006a, b; Jung et al., 2006; 2008; Merikanto et al., 2007; Zhang et al., 2010) and thus a scaling factor of 10^{-5} is applied to the nucleation rate following Jung et al. (2010). The critical nucleus is predicted to consist of roughly two molecules of sulfuric acid and two molecules of ammonia (Napari et al., 2002), so it is assumed here that the newly formed particles consist of ammonium bisulfate and their diameter is 1 nm.

2.2 Gas-phase chemistry

In this work, the simulation of gas phase chemistry in DMAN is updated using the SAPRC99 chemical mechanism (Carter, 2000; Environ, 2003) which includes 211 reactions of 56 gases and 18 free radicals. It includes five lumped alkanes, two lumped olefins, two lumped aromatics, isoprene, a lumped monoterpene, and a lumped sesquiterpene species. Only the two highest molecular weight alkane species are considered as SOA precursors because the other three contain smaller hydrocarbons (Pandis et al., 1991). OLE1 contains all the terminal alkenes, while OLE2 consists of all the internal and cyclic alkenes. The major compounds for each VOC class used in SAPRC99 are listed in Table S1 (Tsimpidi et al., 2010). The nine lumped VOCs are considered as volatile SOA precursors with three of them being biogenic and the rest anthropogenic.

2.3 Coagulation

Coagulation of particles in the atmosphere is an important sink of aerosol number but is also a mechanism by which freshly nucleated particles grow to larger sizes. The TOMAS algorithm is used for the simulation of coagulation. Following Adams and Seinfeld (2002),

185 TOMAS assumes that the aerosol particles coagulate via Brownian diffusion and the effects of
186 gravitational settling and turbulence are negligible. The calculation of the coagulation
187 coefficients is based on the wet diameters of the particles. These wet diameters are calculated
188 following the approach of Gaydos et al. (2005). For small particles (<100 nm), we use the
189 expression of Dahneke et al. (1983) in order to correct for non-continuum effects. The
190 coagulation algorithm uses an adaptive time step. The time step is limited so that the aerosol
191 number or mass concentration in any size category does not increase by more than an order of
192 magnitude or decrease by more than 25%.
193
194 **2.4 Condensation**
195 Condensation of gas-phase species to existing aerosol particles is an important source of
196 aerosol mass and a means by which small particles grow to CCN sizes. The TOMAS algorithm
197 is used for the simulation of condensation/evaporation of sulfuric acid, ammonia and organic
198 vapors, using the wet diameters of the particles (Gaydos et al., 2005). The driving force for
199 condensation of a vapor to an aerosol particle is the difference between its ambient vapor partial
200 pressure and the equilibrium vapor pressure over the particles, or:

201 $$\Delta p_i = p_i - p_i^* x_i(D_p) \exp\left(\frac{4\sigma M_i}{RT\rho D_p}\right) \quad (1)$$

202 where Δp_i is the condensational driving force of the organic vapor i (the difference between the
203 partial pressure of condensing vapor and its equilibrium vapor pressure), p_i is the ambient partial
204 pressure, x_i is the mass fraction of i, p_i^* is the effective saturation pressure over a flat surface, σ is
205 the surface tension, M_i is the molecular weight of i, R is the ideal gas constant, T is the
206 temperature, ρ is the liquid-phase density , and D_p is the diameter of the particle. The exponential
207 term is known as the Kelvin effect due to the curvature of the particles. The exponential term is
208 large for small particles and "prevents" the condensation of organic vapors on these. As a result
209 the Kelvin effect is important for the growth of newly formed particles. We use TOMAS with an
210 adaptive time step to efficiently solve the equations for condensation. The time step is chosen so
211 that individual particles in any size bin do not grow by more than 10%, the partial pressure of the
212 organic vapor does not fall below 25% of its original value, and the time step is never longer
213 than 15 min.

DMANx uses the Pseudo-Steady-State Approximation (PSSA), in which the sulfuric acid concentration is calculated by assuming that its production rate (oxidation of sulfur dioxide) is equal to its consumption rate (condensation and nucleation). Pierce and Adams (2009a) showed that the PSSA for sulfuric acid increases the computational speed with a small loss in accuracy. The PSSA was tested for a variety of conditions ranging from highly polluted to extremely clean conditions. Its predictions for the sulfuric acid vapor concentration and the number of new particles formed during typical atmospheric nucleation events agreed well with the ''benchmark model'' (Pierce and Adams, 2009a). Jung et al. (2010) evaluated the performance of PSSA for sulfuric acid in DMAN against a 4^{th} order Runge-Kutta algorithm and showed that PSSA is accurate and computationally efficient.

Condensation of ammonia is simulated following the approach described by Jung et al. (2006). Ammonia condensation on the ultrafine particles ends when sulfate is fully neutralized to ammonium sulfate. The equilibrium ammonia vapor pressure is assumed to be zero when aerosols are acidic, i.e. when the molar ratio of NH_4^+ to SO_4^{2-} is <2. If the amount of condensed ammonia exceeds the amount needed to neutralize particles during a time step, we limit the maximum amount of ammonia that can condense to avoid numerical problems.

2.5 Secondary organic aerosol formation

Gas-phase oxidation of volatile organic compounds (VOCs) produces semi-volatile products that can then condense to the particle phase. The VBS framework used in DMANx (Donahue et al., 2006) describes the complete volatility range of OA compounds using logarithmically spaced bins, characterized by an effective saturation concentration, C^* (in μg m^{-3}). SOA components partition between the aerosol and gas phases, and can be formed from anthropogenic SOA (aSOA) and biogenic SOA (bSOA) precursors. Each of these types is simulated here with 12 volatility bins (10^{-5}–10^6 μg m^{-3}). We assume an average molecular weight of 200 $gmol^{-1}$ for both aSOA and bSOA, while the effective enthalpies of vaporization are 30 kJ mol^{-1} (Pathak et al., 2007; Stanier et al., 2007). The SOA yields used in the updated version of DMAN are based on the NO_x-dependent stoichiometric yields of Murphy et al. (2009). The partitioning of OA between the gas and particulate phases is approximated using vapor-liquid equilibrium theory (Equation 1).

Semi-volatile and intermediate-volatility organics can be oxidized to species with lower volatility (Donahue et al., 2006) leading to SOA production. The gas-phase chemical aging of SOA precursors is modeled using a second order gas–phase reaction with the hydroxyl radical. We assume that each chemical aging step reduces the volatility of the corresponding organic vapor by one order of magnitude (i.e. shifting organic material from a saturation concentration of e.g. 10^3 to 10^2 μg m^{-3}), with a small net increase in mass (7.5%) to account for the added oxygen. The chemical aging reactions for aSOA precursors are modeled with a rate constant k (298 K) = 1×10^{-11} cm^3 $molec^{-1}$ s^{-1} (Murphy et al., 2009).

In the base case, the gas-phase chemical aging of bSOA precursors is assumed to have a negligible effect on OA concentration (Lane et al., 2008). The oxidation of biogenic VOCs produces semi-volatile organics with saturation concentrations of 1, 10, 10^2 and 10^3 μg m^{-3}. An alternative hypothesis is that the condensation of very low-volatility organics may explain the observed growth. We assume that a small fraction of organics, which are produced from the oxidation of biogenic VOCs, further reacts to form very low-volatility organics with a saturation concentration of $C^* = 10^{-3}$ μg m^{-3} (Pierce et al., 2011). The sensitivity of the model results to this assumption will be tested assuming a reaction converting the gas-phase surrogate species with C^*=1 μg m^{-3} to extremely low volatility SOA with C^*=10^{-3} μg m^{-3} with a reasonable rate constant equal to 1×10^{-11} cm^3 $molec^{-1}$ s^{-1}. The importance of extremely low volatility organic material for the growth of newly formed particles is explored in a subsequent section. This pathway is consistent with the recent observations of extremely low-volatility organic compounds by Ehn et al. (2014), during ozonolysis reactions as well as reactions with the hydroxyl radical.

3. Model Application

We simulated a “typical” spring day with nucleation at both Hyytiala and Finokalia. First, we identified the days with observed particle formation and growth and then averaged the corresponding measurements during these days generating in this way the meteorological and chemical characteristics of an “average” nucleation day for the specific periods in the two locations (April 2007 in Hyytiala and May 2008 in Finokalia). For the parameters for which measurements were not available, but were needed for the model input, (e.g. OH concentration) we followed the same process using the predicted values from the 3-D chemical transport model

PMCAMx (Fountoukis et al., 2015). Results are compared to the corresponding average values observed during the specific periods.

The extended DMAN (DMANx) is first tested in Hyytiala (Finland), an environment dominated by biogenic VOCs. Meteorological data, gas-phase concentrations, and aerosol number distributions are available from ground measurements at the SMEAR II station in Hyytiala and used here as inputs for DMANx. SMEAR II (Station for Measuring Forest Ecosystem–Atmosphere Relations) is located in a rather homogenous Scots pine (*Pinus sylvestris*) stand on flat terrain at the Hyytiala Forestry Field Station of the University of Helsinki ($61^{o}51'$N, $24^{o}17'$E, 181 m above sea level). The biggest city near SMEAR II is Tampere which has approximately 200,000 inhabitants and is located 60 km from the measurement site. Hari and Kulmala (2005) have described the station and its operation in detail. The main inputs of our simulations (Table 1) are meteorological data (temperature and relative humidity), SO_2, NH_3, OH, O_3, VOC concentrations and the initial aerosol number distribution. The SO_2, O_3 concentration, T and RH were measured continuously while the OH concentration was based on the predictions of the 3-D CTM PMCAMx-2008 (Fountoukis et al., 2011). The concentrations of the lumped VOCs, TERP, ISOP and ARO1 were estimated based on Proton Transfer Reaction Mass Spectrometer (PTRMS) measurements. The rest of the lumped VOCs were taken from PMCAMx-2008. The concentration of NH_3 was based on the measurements during the QUEST IV campaign in Hyytiala (Riipinen et al., 2007). The initial aerosol number distributions are available from DMPS (Differential Mobility Particle Sizer) measurements of ambient dry size distributions (Aalto et al., 2001).

DMANx was also tested in Finokalia, a remote area in the Eastern Mediterranean region with high sulfate levels and relatively low VOC concentrations. Finokalia (35^{o} 24′ N, 25^{o} 60′ E) is a remote coastal station located in the southeast of the Mediterranean Sea on the island of Crete in Greece. The nearest large urban center is Heraklion with 150000 inhabitants located 50 km west of Finokalia. The Finokalia station is located at the top of a hill at an elevation of 230 m, facing the sea. There is no notable human activity at a range of approximately 15 km (Kouvarakis et al., 2000). There are very few trees and little vegetation in the surrounding area. Most of the aerosol at the site is transported from the surrounding regions, such as Greece, Turkey and northern Africa (Pikridas et al., 2010). The concentrations of NH_3, SO_2 and aerosol number distributions were based on the measurements during the Finokalia Aerosol

Measurement Experiment -2008 and -2009 (FAME-08 and FAME-09) (Pikridas et al., 2010; 2012). The other inputs (Table 1) were based on the predictions of PMCAMx.

The model simulates a full day beginning at midnight. In each simulation, we assumed that for the initial distribution each size bin contains half organics and half ammonium sulfate. Our results are not especially sensitive to this assumed initial composition; the initial particle size distribution is a lot more critical..

4. Results

4.1 Simulation without condensation of organic vapors

In the simulation neglecting the organic contribution to ultrafine particle growth in Hyytiala the new particles reach a diameter of 9 nm and the growth rate is only 1 nm h^{-1} (Fig. 1a). The typical observed growth rates in Hyytiala are between 1-4.5 nm h^{-1} and the final diameters between 14-45 nm (Pierce et al. 2011; Yli-Juuti et al. 2011). A significant advantage of DMANx is that it can track the composition of fresh particles formed by nucleation. The growing nucleation mode consists of sulfate and ammonium without any organics (Fig. 1b).

In the Finokalia nucleation simulation, the model predicted that the fresh particles grew to 32 nm with a rate of 3 nm h^{-1} (Fig. S1a) which is less than the 5 nm h^{-1} reported by Pikridas et al. (2010; 2012). The particles reached a diameter of 10 nm at 10:00 local time. These new particles consisted of sulfate and ammonium (Fig S1b). At the start of the nucleation event fresh particles consist of 93% sulfate which drops to 72% by the end of the day.

4.2 Organic condensation with σ=0.025 N m^{-1} (no chemical aging of biogenic SOA precursors)

In the simulation with organic vapor condensation and σ=0.025 N m^{-1} (Pierce et al., 2011) without gas-phase chemical aging of biogenic SOA (bSOA) precursors, the predicted growth rate in Hyytiala remains low at 1.2 nm h^{-1} and the diameter of new particles at the end of the day is 12 nm (Fig. 2a) These results are low compared to typical measurements of growth rate in this area. The simulation showed that using a reasonable surface tension value practically prevents the condensation of organics on fresh particles until they can grow above a diameter of 5 nm. Surface tension has also a major effect, as expected, on the composition of the new

particles. At the beginning of the nucleation event (Fig. 2b), the new particles do not contain any organics and their initial growth is due to the condensation of sulfuric acid and ammonia. At 12:00 LST when the new particles have reached a diameter of 5 nm, the effect of surface tension has decreased and organics start slowly condensing, contributing to growth. The mass fraction of organics in the new particles gradually increases reaching 60% at the end of the day when these particles reach 10 nm (Fig. 2b).

The organic composition of the fresh particles in Hyytiala is shown in Figure S2. Components with lower volatility ($C^*=10^{-2}$ and 10^{-3} μg m^{-3}) contribute around 30% of the organic mass in the initial stages of the growth (Fig. S2). Another 55% is due to the $C^*=0.1$ and 1 μg m^{-3} components. As the day goes on the contribution of the more volatile components increases and at the end of the day 65% of the new particle organic mass is semi-volatile material (C^* of 1 and 10 μg m^{-3}). We estimate that the fraction of the condensing organic mass that has gone to the ultrafine particles (diameter <100 nm) reached a maximum value of $3.5x10^{-5}$ at 12:00 LST.

In the case of σ = 0.025 N m^{-1} at Finokalia (without chemical aging of bSOA precursors), the predicted growth rate is 3.8 nm h^{-1} which is still lower than the measured 5 nm h^{-1} rate. The mode diameter of the new particles reaches 42 nm (Fig. S3a). At 9:30 the newly formed particles consist of 90% sulfate, 6% ammonium and 4% organics (Fig. S3b). The organics condensation starts accelerating later, when these particles become larger than 3 nm (after 10:00 LST). The predicted SOA mass fraction increases to 35% by the end of day. The surrogate OA species with $C^*=1$ and 10 μg m^{-3} were the major components of new particles in this case too, representing around 70% of the OA during the day (Fig S4). In this simulation a maximum of 3% of condensing organic mass has gone to the ultrafine particles (at 12:00).

4.3 Contribution of gas-phase chemical aging of biogenic SOA precursors

The simulations described in the previous section (with condensation of organics and σ= 0.025 N m^{-1}) showed that the addition of condensation of semi-volatile organics did not close the gap between predictions and field measurements of particle growth. Adding gas-phase chemical aging of bSOA precursors in the Hyytiala simulation results in a growth rate of 2.2 nm h^{-1} and a final diameter of 23 nm. These are very similar to the values of growth rate (2.1 nm h^{-1}) and final diameter (21 nm) observed in Hyytiala on 10 April 2007 (Pierce et al., 2011) (Fig. 3). In the

beginning of the simulation the new particles consist mainly of ammonium sulfate and a small amount of organics (Fig. 4a). This small fraction of organics is the extremely low-volatility organics ($C^*= 10^{-3}$ μg m^{-3}) produced from the aging reaction of bSOA precursors (Fig. 4b). During the day the new particles grow and the mass of organics increase. The low volatility material dominates the growth during the first few hours when the diameter is less than 5 nm, while the semi-volatile ($C^*= 1$, 10 and 100 μg m^{-3}) dominates the growth during the later stages. At 18:00 LST the new particles consist mostly (90%) of organics (40% of low volatility and 60% semi-volatile SOA) (Fig 4). The semi-volatile SOA contributes to growth when the particles pass the size of ~10 nm where the Kelvin effect is small. The aging reaction affects new particles at the beginning of growth when the particles are very small. The maximum mass of condensing organics that has gone to the ultrafine particles is about 0.9 % at noon which is larger than in the simulation without aging.

The assumed gas-phase aging reaction of bSOA precursors helps new particles to grow to larger sizes in Finokalia too and predictions are now consistent with field measurements (Fig. 5). The predicted growth rate is 4.7 nm h^{-1} while the measured growth rate in Finokalia is around 5 nm h^{-1} (Pikridas et al., 2012). The revised model can reproduce the observed growth rate and the final particle size encouragingly well. At the start of the growth, the new particles consist of 85% $(NH_4)_2SO_4$ while at the end of the day this drops to 55% (Fig. 6a). The organic components initially comprise 12% of the nucleated particle mass, and are mostly of low volatility (75% is from the $C^* = 10^{-3}$ μg m^{-3} volatility bin). During the day the organics mass fraction increases, reaching a maximum of 45% of the nucleated particle mass and consisting of 30% low-volatility and 70% semi-volatile organics (Fig. 6b). 4% of the condensing organics at noon has gone to the ultrafine particles.

4.4 Sensitivity analysis

4.4.1 Organic condensation neglecting the Kelvin effect without aging of bSOA precursors

Condensation of organics neglecting the Kelvin effect (assuming $\sigma = 0$ N m^{-1}) helps the newly formed particles to reach a diameter of 28 nm in Hyytiala while the average growth rate is 1.8 nm h^{-1} (Fig. S5a). At 8:00 LST the nucleation mode particles have a size of ~2 nm and consist of 55% sulfate, 11% ammonium and 34% organics. During the day the new particles continue to grow and the fraction of organics increases to 85% at the end of the day (Fig. S5b).

The size of the new particles increases due to the condensation of organics. The surrogate OA components with effective saturation concentration of C^*= 1 and 10 μg m^{-3} are predicted to be the major components of the fresh particles contributing 80% of the SOA, initially, and 70% in the end (Fig. S6).

For the Finokalia case, the predicted growth rate of new particles is 3.8 nm h^{-1} and the diameter of the new fresh particles reaches 42 nm (Fig. S7a). The condensation of organics helps the particles to grow faster and to reach larger sizes compared to the case described in 4.1. At 8:00 the particles consist of 35% organics, 5% ammonium and 60% sulfate (Fig. S7b). After 11:00 the new particles composition is relatively stable: 40% organics, 42% sulfate and 18% ammonium. For this case of zero surface tension, organics condense immediately on the newly formed particles, resulting in fast growth. In this case about 6.5% of condensing organics has gone to the ultrafines at 12:00. The SOA composition is similar to that of the σ= 0.025 N m^{-1} case (Fig S8).

4.4.2 Sensitivity of particle number concentration to surface tension

So far the model showed that organic condensation can cause an increase in the size of the ultrafine particles. However, large particles also grow by organic condensation resulting in increased coagulation probability for the newly formed particles (Kuang et al., 2009; Westervelt et al., 2013; 2014). This causes a significant reduction in the number concentration of small particles compared to the case without condensation of organics. The increase of surface tension leads to organic vapor condensation mostly on large particles and to a smaller extent on freshly nucleated particles due to the increased Kelvin effect which prevents the condensation of organics on new particles.

The predicted daily mean number concentration of particles above 3 nm (N_3) in Hyytiala is 3100 cm^{-3} for the simulation without organics, 5400 cm^{-3} for the zero surface tension case, 2500 cm^{-3} when the organic surface tension is 0.025 N m^{-1} and 3,000 cm^{-3} with the aging of bSOA precursors (Fig. 7a). The maximum value of N_3 is predicted at 13:00 in all cases. For the zero surface tension simulation $N_{3,max}$ is 13500 cm^{-3} while in the no-organics case $N_{3,max}$=6300 cm^{-3}. When the organic surface tension is 0.025 N m^{-1} $N_{3,max}$=4600 cm^{-3} and increases to 6000 cm^{-3} with the addition of aging of bSOA precursors (Fig. 7a).

427 At Finokalia the average predicted daily concentration of N_3 is 3600 cm^{-3} without the
428 condensation of organics and is predicted to be the same for the bSOA aging case. A similar N_3
429 is predicted for the σ=0.025 N m^{-1} case (3,550 cm^{-3}) (Fig. S9a) while N_3 increases to 4300 cm^{-3}
430 for zero surface tension. The maximum N_3 is predicted to be the largest for the zero surface
431 tension case (Fig. S9a).
432 Neglecting the Kelvin effect in both locations allows rapid condensation of organics on
433 the fresh particles resulting in an increase of N_3. The Kelvin effect prevents the condensation of
434 organics on new particles resulting in a decrease of N_3. The bSOA aging and the σ=0.025 N m^{-1}
435 simulations do not significantly affect N_3 compared to the simulation without organics.
436 The daily mean number concentration of particles above 100 nm (N_{100}) in Hyytiala is 380
437 cm^{-3} for the no-organics case and 440 cm^{-3} for all the other simulations (Fig. 7b). In all the
438 Hyytiala simulations with organics condensing N_{100} increases after 8:00 due to organics while in
439 the simulation without organics a smaller increase is predicted after 12:00 due to sulfuric acid
440 (Fig. 7b). Condensation of organics increased N_{100} by 25% at the end of the day.
441 A similar behavior is predicted at Finokalia. N_{100} starts increasing after 8:00 for all the
442 cases with organics condensation and after 9:00 for the no-organics case. The reason for the
443 shorter delay before the onset of N_{100} increase in the no-organics case compared to Hyytiala is
444 that the condensation of sulfuric acid-ammonium has a predominant role in Finokalia at
445 increasing N_{100} while at Hyytiala simulations organics dominate this growth process.
446 Furthermore, at Finokalia the concentration of sulfuric acid is higher and the photochemistry is
447 faster (much higher OH levels) than at Hyytiala. The daily mean number concentration of
448 particles that can act as CCN (N_{100}) is predicted to be 1000 cm^{-3} without organics and 1100 cm^{-3}
449 for the other simulations (Fig. S9b). N_{100} reaches a maximum (1070 cm^{-3}) at 13:00 for the no-
450 organics case and at 18:00 in the other simulations (1210 cm^{-3}) (Fig. S9b). At the end of the day
451 N_{100} has increased by 13% due to condensation of organics. The increase of surface tension and
452 the addition of aging of bSOA precursors do not change N_{100}.
453

454 ## 5. Conclusions

455 We developed an updated version of DMAN (DMANx) which includes the condensation
456 of organic vapors on ultrafine particles, using the Volatility Basis Set framework. Simulations

were performed for two locations with different organic sources, Hyytiala and Finokalia, during a typical springtime day with aerosol nucleation and growth.

Using realistic values of surface tension we estimate that the semi-volatile organics condensation is not enough to grow the new particles to sizes comparable to those observed. Assuming that biogenic SOA precursors chemically age and produce extremely low volatility organics (i.e. with an effective saturation concentration of 10^{-3} μg m^{-3}) results in predicted growth rates similar to those measured. In the biogenic VOC-dominated environment of Hyytiala, the very low volatility organics condense onto particles smaller than 3 nm. After this first-stage of growth for the new particles, the Kelvin effect becomes small and the semi-volatile organics are the major components controlling the subsequent growth of the nucleated particles. In an environment with more sulfuric acid and less biogenic VOCs (Finokalia) the condensation of organics plays a complementary role in the growth of nucleated particles contributing 45% of the total mass of new particles during a day representative of springtime nucleation.

The gas-phase chemical aging of biogenic SOA precursors contributes to the growth of the nucleated particles because of the extra mass added from the aging reactions. Laboratory experiments and direct field measurements (Ehn et al., 2014) support the importance of extremely low-volatility VOCs produced in the gas phase from the oxidation of monoterpenes and other VOCs.

The condensation of organics with zero surface tension resulted in a predicted growth rate similar to the field measurements, but the zero value of surface tension is unrealistic. The condensation of organics with zero surface energy also affects the number concentration of particles. Increasing surface tension inhibits the growth of new fresh particles and thus results in a decrease of total particle number concentrations in both locations. Interestingly, when including aging of bSOA precursors the new model predicts daily mean number concentrations similar to those for the no-organics simulation. The number concentration of particles that can act as CCN (N_{100}) increases (by 13% at Finokalia and 25% at Hyytiala) during a typical spring day with nucleation, compared to the case in which the condensation of organics is neglected. The increase of surface tension and the aging of bSOA precursors do not significantly affect N_{100} compared to the zero surface energy case.

Acknowledgements: We thank Prof. Kulmala and the U. of Helsinki team for the Hyytiala measurements. This work was funded by the ARISTEIA project (National Research Excellence Grant) and the ATMOPACS project (grant agreement 267099).

6. References

Aalto, P., Hameri, K., Becker, E., Weber, R., Salm. J., Makela, J. M., Hoell, C., O'Dowd, C., Karlsson, H., Hansson, H. C., Vakeva, M., Koponen, I., Buzorius, G., and Kulmala, M.: Physical characterization of aerosol particles during nucleation events, Tellus, 53B, 344–358, 2001.

Adams, P.J., and Seinfeld, J. H.: Predicting global aerosol size distributions in general circulation models, J. Geophys. Res., 107, doi:10.1029/2001JD001010, 2002.

Albrecht, B.A.: Aerosols, cloud microphysics, and fractional cloudiness, Science 245, 1227–1230, 1989.

Atkinson, R.: Atmospheric chemistry of VOCs and NO_x, Atmos. Environ., 34, 2063–2101, 2000.

Atkinson, R., and Arey, J.: Atmospheric degradation of volatile organic compounds, Chem. Rev., 103, 4605–4638, 2003.

Almeida, J., Schobesberger, S., Kurten, A., Ortega, I. K., Kupiainen-Maatta, O., Praplan, A. P., Adamov, A., Amorim, A., Bianchi, F., Breitenlechner, M., David, A., Dommen, J., Donahue, N. M., Downard, A., Dunne, E., Duplissy, J., Ehrhart, S., Flagan, R. C., Franchin, A., Guida, R., Hakala, J., Hansel, A., Heinritzi, M., Henschel, H., Jokinen, T., Junninen, H., Kajos, M., Kangasluoma, J., Keskinen, H., Kupc, A., Kurten, T., Kvashin, A. N., Laaksonen, A., Lehtipalo, K., Leiminger, M., Leppa, J., Loukonen, V., Makhmutov, V., Mathot, S., McGrath, M. J., Nieminen, T., Olenius, T., Onnela, A., Petaja, T., Riccobono, F., Riipinen, I., Rissanen, M., Rondo, L., Ruuskanen, T., Santos, F. D., Sarnela, N., Schallhart, S., Schnitzhofer, R., Seinfeld, J. H., Simon, M., Sipila, M., Stozhkov, Y., Stratmann, F., Tome, A., Trostl, J., Tsagkogeorgas, G., Vaattovaara, P., Viisanen, Y., Virtanen, A., Vrtala, A., Wagner, P. E., Weingartner, E., Wex, H., Williamson, C., Wimmer, D., Ye, P., Yli-Juuti, T., Carslaw, K. S., Kulmala, M., Curtius, J., Baltensperger, U., Worsnop, D. R., Vehkamaki, H., and Kirkby, J.: Molecular understanding of sulphuric acid-amine particle nucleation in the atmosphere, Nature, 502, 359-363, 2013.

517 Anttila, T., and Kerminen, V.: Condensational growth of atmospheric nuclei by organic vapours,
518 J. Aerosol Sci., 34, 41–61, 2003.
519 Berndt, T., Stratmann, F., Sipilä, M., Vanhanen, J., Petäjä, T., Mikkilä, J., Grüner, A.,
520 Spindler, G., Lee Mauldin III, R., Curtius, J., Kulmala, M., and Heintzenberg, J.: Laboratory
521 study on new particle formation from the reaction OH + SO_2: influence of experimental
522 conditions, H_2O vapour, NH_3 and the amine tert-butylamine on the overall process, Atmos.
523 Chem. Phys., 10, 7101-7116, doi:10.5194/acp-10-7101-2010, 2010.
524 Bonn, B., Kulmala, M., Riipinen, I., Sihto, S. L., and Ruuskanen, T. M.: How biogenic terpenes
525 govern the correlation between sulfuric acid concentrations and new particle formation, J.
526 Geophys. Res., 113, doi:10.1029/2007JD009327, 2008.
527 Carter, W. P. L.: Programs and files implementing the SAPRC-99 mechanism and its associated
528 emissions processing procedures for Models-3 and other regional models, January 31, 2000.
529 Coffman, D.J., and Hegg, D.A.: A preliminary study of the effect of ammonia on particle
530 nucleation in the MBL, J. Geophys. Res., 100, 7147–7160, 1995.
531 Dahneke, B.: Simple kinetic theory of Brownian diffusion in vapors and aerosols, in Theory of
532 Dispersed Multiphase Flow, edited by R. E. Meyer, 97–138, Academic, San Diego, Calif.,
533 1983.
534 Donaldson, K., Li, X.Y., and Mac Nee, W.: Ultrafine (nanometer) particle mediated lung injury,
535 J. Aerosol Sci., 29, 553–560, 1998.
536 Donaldson, K., Brown, D., Clouter, A., Duffin, R., MacNee, W., Renwick, L., Tran, L., and
537 Stone, V.: The pulmonary toxicology of ultrafine particles, Journal of Aerosol Medicine, 15,
538 213–220, 2002.
539 Donahue, N. M., Robinson, A. L., Stanier, C. O., and Pandis, S. N.: Coupled partitioning,
540 dilution, and chemical aging of semivolatile organics, Environ. Sci. Technol., 40, 2635–
541 2643, 2006.
542 Dusek, U., Frank, G. P., Hildebrandt, L., Curtius, J., Schneider, J., Walter, S., Chand, D.,
543 Drewnick, F., Hings, S., Jung, D., Borrmann, S., and Andreae, M. O.: Size matters more
544 than chemistry for cloud-nucleating ability of aerosol particles, Science, 312, 1375–1378,
545 2006.
546 Ehn, M., Thornton, J. A., Kleist, E., Sipilä, M., Junninen, H., Pullinen, L., Springer, M., Rubach,
547 F., Tillmann, R., Lee, B., Lopez-Hilfiker, F., Andres, S., Acir, I.-H., Rissanen, M., Jokinen,

548 T., Schobesberger, S., Kangasluoma, J., Kontkanen, J., Nieminen, T., Kurtén, T., Nielsen, L.
549 B., Jørgensen, S., Kjaergaard, G. H., Canagaratna, M., Dal Maso, M., Berndt, T., Petäjä, T.,
550 Wahner, A., Kerminen, V.-M., Kulmala, M., Worsnop, D. R., Wildt, J., and Mentel, T. F.: A
551 large source of low-volatility secondary organic aerosol. Nature, 506,
552 doi:10.1038/nature13032, 2014.
553 Eisele, F. L. and McMurry, P. H.: Recent progress in understanding particle nucleation and
554 growth, Phil. Trans. R. Soc. Lond., 352, 191-201, 1997.
555 Environ, User's guide to the comprehensive air quality model with extensions (CAMx), version
556 4.02, report, ENVIRON Int. Corp., Novato, Calif, 2003.
557 Fountoukis, C., Racherla, P. N., Denier van der Gon, H. A. C., Polymeneas, P., Charalampidis,
558 P. E., Pilinis, C., Wiedensohler, A., Dall'Osto, M., O'Dowd, C., and Pandis, S. N.:
559 Evaluation of a three-dimensional chemical transport model (PMCAMx) in the European
560 domain during the EUCAARI May 2008 campaign, Atmos. Chem. Phys., 11, 10331–10347,
561 2011.
562 Fountoukis, C., Riipinen, I., Denier van der Gon, H. A. C., Charalampidis, P. E., Pilinis, C.,
563 Wiedensohler, A., O'Dowd, C., Putaud, J. P., Moerman, M., and Pandis, S. N.: Simulating
564 ultrafine particle formation in Europe using a regional CTM: contribution of primary
565 emissions versus secondary formation to aerosol number concentrations, Atmos. Chem.
566 Phys., 12, 8663-8677, 2012.
567 Gaydos, T.M., Stainer, C.O., and Pandis, S.N.: Modeling of in situ ultrafine atmospheric particle
568 formation in the eastern United State, J. Geophys. Res., 110, doi:10.1029/2004JD004683,
569 2005.
570 Gaydos, T., Pinder, R., Koo, B., Fahey, K., Yarwood, G., and Pandis, S. N.: Development and
571 application of a three-dimensional Chemical Transport Model, PMCAMx, Atmos. Environ.,
572 41, 2594–2611, 2007.
573 Godleski, J. J., Verrier, R. L., Koutrakis, P., Catalano, P., Coull, B., Reinisch, U., Lovett, E. G.,
574 Lawrence, J., Murthy, G. G., Wolfson, J. M., Clarke, R. W., Nearing, B. D., and
575 Killingsworth, C.: Mechanisms of morbidity and mortality from exposure to ambient air
576 particles, Res. Rep. Health Eff. Inst., 91, 5–103, 2000.
577 Goldstein, A. H. and Galbally, I. E.: Known and unexplored organic constituents in the earth's
578 atmosphere, Environ. Sci. Technol., 41, 1514–1521, 2007.

579 Hallquist, M., Wenger, J. C., Baltensperger, U., Rudich, Y., Simpson, D., Claeys, M., Dommen,
580 J., Donahue, N. M., George, C., Goldstein, A. H., Hamilton, J. F., Herrmann, H., Hoffmann,
581 T., Iinuma, Y., Jang, M., Jenkin, M. E., Jimenez, J. L., Kiendler-Scharr, A., Maenhaut, W.,
582 McFiggans, G., Mentel, Th. F., Monod, A., Prevt, A. S. H., Seinfeld, J. H., Surratt, J. D.,
583 Szmigielski, R., and Wildt, J.: The formation, properties and impact of secondary organic
584 aerosol: current and emerging issues, Atmos. Chem. Phys., 9, 5155–5236, 2009.
585 Hari, P. and Kulmala, M.: Station for measuring ecosystem atmosphere relations (SMEAR II),
586 Boreal Env. Res., 10, 315–322, 2005.
587 Hildebrandt, L., Donahue, N. M., and Pandis, S. N.: High formation of secondary organic aerosol
588 from the photo-oxidation of toluene, Atmos. Chem. Phys., 9, 2973–2986, 2009.
589 Hoffmann, T., O'Dowd, C.D., and Seinfeld, J. H.: Iodine oxide homogeneous nucleation: an
590 explanation for coastal new particle production, Geophys. Res. Let., 28, 1949–1952, 2001.
591 Janson, R., Rosman, K., Karlsson, A., and Hansson, H. C.: Biogenic emissions and gaseous
592 precursors to forest aerosols, Tellus B, 53, 423–440, 2001.
593 Jimenez, J. L., Canagaratna, M. R., Donahue, N. M., Prevot, A. S. H., Zhang, Q., Kroll, J. H.,
594 DeCarlo, P. F., Allan, J. D., Coe, H., Ng, N. L., Aiken, A. C., Docherty, K. S., Ulbrich, I.
595 M., Grieshop, A. P., Robinson, A. L., Duplissy, J., Smith, J. D., Wilson, K. R., Lanz, V. A.,
596 Hueglin, C., Sun, Y. L., Tian, J., Laaksonen, A., Raatikainen, T., Rautiainen, J.,
597 Vaattovaara, P., Ehn, M., Kulmala, M., Tomlinson, J. M., Collins, D. R., Cubison, M. J., E,
598 Dunlea, J., Huffman, J. A., Onasch, T. B., Alfarra, M. R., Williams, P. I., Bower, K., Kondo,
599 Y., Schneider, J., Drewnick, F., Borrmann, S., Weimer, S., Demerjian, K., Salcedo, D.,
600 Cottrell, L., Griffin, R., Takami, A., Miyoshi, T., Hatakeyama, S., Shimono, A., Sun, J. Y.,
601 Zhang, Y. M., Dzepina, K., Kimmel, J. R., Sueper, D., Jayne, J. T., Herndon, S. C.,
602 Trimborn, A. M., Williams, L. R., Wood, E. C., Middlebrook, A. M., Kolb, C. E.,
603 Baltensperger, U., and Worsnop, D. R.: Evolution of organic aerosols in the atmosphere,
604 Science, 326, 1525–1529, 2009.
605 Jung, J., Adams, P. J., and Pandis, S. N.: Simulating the size distribution and chemical
606 composition of ultrafine particles during nucleation events, Atmos. Environ., 40, 2248–
607 2259, 2006.
608 Jung, J., Adams, P. J., and Pandis, S. N.: Evaluation of nucleation theories in a sulfur-rich
609 environment, Aerosol Sci. Technol., 42, 495–504, 2008.

610 Jung, J., Fountoukis, C., Adams, P. J., and Pandis, S. N.: Simulation of in situ ultrafine particle
611 formation in the eastern United States using PMCAMx-UF, J. Geophys. Res., 115,
612 doi:10.1029/2009JD012313, 2010.
613 Kanakidou, M., Seinfeld, J. H., Pandis, S. N., Barnes, I., Dentener, F. J., Facchini, M. C., Van
614 Dingenen, R., Ervens, B., Nenes, A., Nielsen, C. J., Swietlicki, E., Putaud, J. P., Balkanski,
615 Y., Fuzzi, S., Horth, J., Moortgat, G. K., Winterhalter, R., Myhre, C. E. L., Tsigaridis, K.,
616 Vignati, E., Stephanou, E. G., and Wilson, J.: Organic aerosol and global climate modelling:
617 a review, Atmos. Chem. Phys., 5, 1053–1123, 2005.
618 Karydis, V. A., Tsimpidi, A. P., and Pandis, S. N.: Evaluation of a three-dimensional chemical
619 transport model (PMCAMx) in the eastern United States for all four seasons, J. Geophys.
620 Res., 112, doi:10.1029/2006JD007890, 2007.
621 Kerminen, V. M., Virkkula, A., Hillamo, R., Wexler, A. S., and Kulmala, M.: Secondary
622 organics and atmospheric cloud condensation nuclei production, J. Geophys. Res., 105,
623 9255–9264, 2000.
624 Kerminen, V. M., Pirjola, L., and Kulmala, M.: How significantly does coagulational scavenging
625 limit atmospheric particle production?, J. Geophys. Res., 106, 24119–24125, 2001.
626 Kerminen, V. M., Lihavainen, H., Komppula, M., Viisanen, Y., and Kulmala, M.: Direct
627 observational evidence linking atmospheric aerosol formation and cloud droplet activation,
628 Geophys. Res. Lett., 32, doi:10.1029/2005GL023130, 2005.
629 Kirkby, J. et al.: Role of sulphuric acid, ammonia and galactic cosmic rays in atmospheric
630 aerosol nucleation, Nature, 476, 429–433, 2011.
631 Korhonen, P., Laaksonen, A., Viisanen, Y., McGraw, R., and Seinfeld, J. H.: Ternary nucleation
632 of H_2SO_4, NH_3, and H_2O in the atmosphere, J. Geophys. Res., 104, 26349–26353, 1999.
633 Kouvarakis, G., Tsigaridis, K., Kanakidou, M., and Mihalopoulos, N.: Temporal variations of
634 surface regional background ozone over Crete Island in the southeast Mediterranean, J.
635 Geophys. Res., 105, 4399–4407, 2000.
636 Kuang, C., McMurry, P. H., McCormick, A. V., and Eisele, F. L.: Dependence of nucleation
637 rates on sulfuric acid vapor concentration in diverse atmospheric locations, J. Geophys. Res.,
638 113, doi:10.1029/2007JD009253, 2008.

639 Kuang, C., McMurry, P. H., and McCormick, A. V.: Determination of cloud condensation nuclei
640 production from measured new particle formation events, Geophys. Res. Lett., 36, L09822,
641 doi:10.1029/2009GL037584, 2009.
642 Kulmala, M., Pirjola, L., and Makela, J. M.: Stable sulphate clusters as a source of new
643 atmospheric particles, Nature 404, 66–69, 2000.
644 Kulmala, M., Korhonen, P., Napari, I., Karlsson, A., Berresheim, H., and O'Dowd, C. D.:
645 Aerosol formation during PARFORCE: ternary nucleation of H_2SO_4, NH_3, and H_2O, J.
646 Geophys. Res., 107, doi:10.1029/2001JD000900, 2002.
647 Kulmala, M., Vehkamaki, H., Petaja, T., Dal Maso, M., Lauri, A., Kerminen, V.-M., Birmili, W.,
648 and McMurry, P. H.: Formation and growth of ultrafine atmospheric particles: A review of
649 observations, J. Aerosol Sci., 35, 143–176, 2004.
650 Kurten, T., Loukonen, V., Vehkamaki, H., and Kulmala, M.: Amines are likely to enhance
651 neutral and ion-induced sulfuric acid-water nucleation in the atmosphere more effectively
652 than ammonia, Atmos. Chem. Phys., 8, 4095–4103, 2008.
653 Laakso, L., Makela, J. M., Pirjola, L., and Kulmala, M.: Model studies on ion – induced
654 nucleation in the atmosphere, J. Geophys. Res., 107, doi:10.1029/2002JD002140, 2002.
655 Laaksonen, A., Hamed, A., Joutsensaari, J., Hiltunen, L., Cavalli, F., Junkermann, W., Asmi, A.,
656 Fuzzi, S., and Facchini, M. C.: Cloud condensation nucleus production from nucleation
657 events at a highly polluted region, Geophys. Res. Lett., 32, doi:10.1029/2004GL022092,
658 2005.
659 Lane, T. E., Donahue, N. M., and Pandis, S. N.: Simulating secondary organic aerosol formation
660 using the volatility basis-set approach in a chemical transport model, Atmos. Environ., 42,
661 7439–7451, 2008.
662 Lihavainen, H., Kerminen, V. M., Komppula, M., Hatakka, J., Aaltonen, V., Kulmala, M., and
663 Viisanen, Y.: Production of “potential” cloud condensation nuclei associated with
664 atmospheric new particle formation in northern Finland, J. Geophys. Res., 108,
665 doi:10.1029/2003JD003887, 2003.
666 Makkonen, R., Asmi, A., Korhonen, H., Kokkola, H., Jarvenoja, S.,Raisanen, P., Lehtinen, K. E.
667 J., Laaksonen, A., Kerminen, V. M., Jarvinen, H., Lohmann, U., Bennartz, R., Feichter, J.,
668 and Kulmala, M.: Sensitivity of aerosol concentrations and cloud properties to nucleation

669 and secondary organic distribution in ECHAM5-HAM global circulation model, Atmos.
670 Chem. Phys., 9, 1747–1766, 2009.
671 Marti, J. J., Weber, R. J., McMurry, P. H., Eisele, F., Tanner, D., and Jefferson, A.: New particle
672 formation at a remote continental site, assessing the contributions of SO_2 and organic
673 precursors, J. Geophys. Res., 102, 6331–6339, 1997.
674 Merikanto, J., Napari, I., Vehkamaki, H, Anttila, T., and Kulmala, M.: New parameterization of
675 sulfuric acid-ammonia-water ternary nucleation rates at tropospheric conditions, J. Geophys.
676 Res., 112, doi:10.1029/2006JD007977, 2007.
677 Merikanto, J., Spracklen, D. V., Mann, G. W., Pickering, S. J., and Carslaw, K. S.: Impact of
678 nucleation on global CCN, Atmos. Chem. Phys., 9, 8601–8616, 2009.
679 Metzger, A., Verheggen, B., Dommen, J., Duplissy, J., Prevot, A. S. H., Weingartner, E.,
680 Riipinen, I., Kulmala, M., Spracklen, D. V., Carslaw, K. S., and Baltensperger, U.: Evidence
681 for the role of organics in aerosol particle formation under atmospheric conditions, Proc.
682 Natl. Acad. Sci., 107, 6646–6651, 2010.
683 Murphy, B. N. and Pandis, S.N.: Simulating the formation of semivolatile primary and secondary
684 organic aerosol in a regional chemical transport model, Environ. Sci. Technol., 43, 4722–
685 4728, 2009.
686 Napari, I., Noppel, M., Vehkamaki, H., and Kulmala, M.: Parameterization of ternary nucleation
687 rates for H_2SO_4-NH_3-H_2O vapors, J. Geophys. Res., 107, doi:10.1029/2002JD002132, 2002.
688 Ng, N. L., Kroll, J. H., Keywood, M. D., Bahreini, R., Varutbangkul, V., Flagan, R. C., Seinfeld,
689 J. H., Lee, A. and Goldstein, A. H.: Contributions of first- versus second-generation
690 products to secondary organic aerosols formed in the oxidation of biogenic hydrocarbons,
691 Environ. Sci. Technol., 40, 2283–2297, 2006.
692 Nieminen, N., Manninen, H. E., Sihto, S. L., Yli-Juuti, T., Mauldin, R. L., Petaja, T., Riipinen, I.,
693 Kerminen, V.-M., and Kulmala, M.: Connection of sulfuric acid to atmospheric nucleation
694 in boreal forest, Environ. Sci. Technol., 43, 4715–4721, 2009.
695 Nilsson, E.D., and Kulmala, M.: The potential for atmospheric mixing processes to enhance the
696 binary nucleation rate, J. Geophys. Res., 103, 1381–1389, 1998.
697 Odum, J. R., Hoffman, T., Bowman, F., Collins, D., Flagan, R. C., and Seinfeld, J. H.:
698 Gas/particle partitioning and secondary organic aerosol yields. Environ. Sci. Technol., 30,
699 2580–2585, 1996.

700 Paasonen, P., Sihto, S. L., Nieminen, T., Vuollekoski, H., Riipinen, I., Plass-Dulmer, C.,
701 Berresheim, H., Birmili, W., and Kulmala, M.: Connection between new particle formation
702 and sulphuric acid at Hohenpeissenberg (Germany) including the influence of organic
703 compounds, Boreal Environ. Res., 14, 616–629, 2009.
704 Paasonen, P., Nieminen, T., Asmi, E., Manninen, H. E., Petaja, T., Plass-Dulmer, C., Flentje, H.,
705 Birmili, W., Wiedensohler, A., Horrak, U., Metzger, A., Hamed, A., Laaksonen, A.,
706 Facchini, M. C., Kerminen, V.-M., and Kulmala, M.: On the roles of sulphuric acid and low-
707 volatility organic vapours in the initial steps of atmospheric new particle formation, Atmos.
708 Chem. Phys., 10, 11223–11242, 2010.
709 Pandis, S. N., Paulson, S. E., Seinfeld, J. H., and Flagan, R.C.: Aerosol formation in the
710 photooxidation of isoprene and α-pinene, Atmos. Environ., 25A, 997–1008, 1991.
711 Pandis, S. N., Donahue, N. M., Murphy, B. N., Riipinen, I., Fountoukis, C., Karnezi, E., Patoulias,
712 D., and Skyllakou, K.: Atmospheric organic aerosols: insights from the combination of
713 measurements chemical transport models, Faraday Discuss., doi:10.1039/c3fd00108c, 2013.
714 Pathak, R. K., Presto, A. A., Lane, T. E., Stanier, C. O., Donahue, N. M., and Pandis, S. N.:
715 Ozonolysis of R-pinene: parameterization of secondary organic aerosol mass fraction,
716 Atmos. Chem. Phys., 7, 3811–3821, 2007.
717 Peters, A., Wichmann, H. E., Tuch T., Heinrich J., and Heyder J.: Respiratory effects are
718 associated with the number of ultrafine particles, Am. J. Respir. Crit. Care Med., 155, 1376–
719 1383, 1997.
720 Presto, A. A., Donahue, N. M.: Investigation of α-pinene + ozone secondary organic aerosol
721 formation at low total aerosol mass, Environ. Sci. Technol., 40, 3536–3543, 2006.
722 Pierce, J. R. and Adams, P. J.: A computationally efficient aerosol nucleation/condensation
723 method: Pseudo-steady state sulfuric acid, Aerosol Sci. Technol., 43, 216–226, 2009a.
724 Pierce, J. R. and Adams, P. J.: Uncertainty in global CCN concentrations from uncertain aerosol
725 nucleation and primary emission rates, Atmos. Chem. Phys., 9, 1339–1356, 2009b.
726 Pierce, J. R., Riipinen, I., Kulmala, M., Ehn, M., Petaja, T., Junninen, H., Worsnop, D. R., and
727 Donahue, N. M.: Quantification of the volatility of secondary organic compounds in
728 ultrafine particles during nucleation events, Atmos. Chem. Phys., 11, 9019–9036, 2011.
729 Pirjola, L., and Kulmala, M.: Development of particle size and composition distributions with a
730 novel aerosol dynamics model, Tellus B, 53, 491–509, 2001.

731 Pikridas, M., Bougiatioti, A., Hildebrandt, L., Engelhart, G. J., Kostenidou, E., Mohr, C.,
732 Prévôt, A. S. H., Kouvarakis, G., Zarmpas, P., Burkhart, J. F., Lee, B.-H., Psichoudaki, M.,
733 Mihalopoulos, N., Pilinis, C., Stohl, A., Baltensperger, U., Kulmala, M., and Pandis, S. N.:
734 The Finokalia Aerosol Measurement Experiment – 2008 (FAME-08): an overview, Atmos.
735 Chem. Phys., 10, 6793-6806, 2010.
736 Pikridas M., Riipinen, I., Hildebrandt, L., Kostenidou, E., Manninen, H., Mihalopoulos, N.,
737 Kalivitis, N., Burkhart, J. F., Stohl, A., Kulmala, M., and Pandis, S. N.: New particle
738 formation at a remote marine site in the Eastern Mediterranean, J. Geophys. Res., 117,
739 doi:10.1029/2012JD017570, 2012.
740 Riccobono, F., Schobesberger, S., Scott, C. E., Dommen, J., Ortega, I. K., Rondo, L., Almeida,
741 J., Amorim, A., Bianchi, F., Breitenlechner, M., David, A., Downard, A., Dunne, E. M.,
742 Duplissy, J., Ehrhart, S., Flagan, R. C., Franchin, A., Hansel, A., Junninen, H., Kajos, M.,
743 Keskinen, H., Kupc, A., Kürten, A., Kvashin, A. N., Laaksonen, A., Lehtipalo, K.,
744 Makhmutov, V., Mathot, S., Nieminen, T., Onnela, A., Petäjä, T., Praplan, A. P., Santos, F.
745 D., Schallhart, S., Seinfeld, J. H., Sipilä, M., Spracklen, D. V., Stozhkov, Y., Stratmann, F.,
746 Tomé, A., Tsagkogeorgas, G., Vaattovaara, P., Viisanen, Y., Vrtala, A., Wagner, P. E.,
747 Weingartner, E., Wex, H., Wimmer, D., Carslaw, K. S., Curtius, J., Donahue, N. M.,
748 Kirkby, J., Kulmala, M., Worsnop, D. R., and Baltensperger, U.: Oxidation products of
749 biogenic emissions contribute to nucleation of atmospheric particles, Science, 344, 717-
750 721, 2014.
751 Riipinen, I., Sihto, S.-L., Kulmala, M., Arnold, F., Dal Maso, M., Birmili, W., Saarnio, K.,
752 Teinila, K., Kerminen, V.-M., Laaksonen, A., and Lehtinen, K. E. J.: Connections between
753 atmospheric sulphuric acid and new particle formation during QUEST III–IV campaigns in
754 Heidelberg and Hyytiala, Atmos. Chem. Phys., 7, 1899–1914, 2007.
755 Riipinen, I., Pierce, J. R., Yli-Juuti, T., Nieminen, T., Hakkinen, S., Ehn, M., Junninen, H.,
756 Lehtipalo, K., Petaja, T., Slowik, J., Chang, R., Shantz, N. C., Abbatt, J., Leaitch, W. R.,
757 Kerminen, V.-M., Worsnop, D. R., Pandis, S. N., Donahue, N. M., and Kulmala, M.:
758 Organic condensation: a vital link connecting aerosol formation to cloud condensation
759 nuclei (CCN) concentrations, Atmos. Chem. Phys., 11, 3865–3878, 2011.
760 Sihto, S. L., Kulmala, M., Kerminen, V. M., Dal Maso, M., Petaja, T., Riipinen, I., Korhonen,
761 H., Arnold, F., Janson, R., Boy, M., Laaksonen, A., and Lehtinen, K. E. J.: Atmospheric

762 sulphuric acid and aerosol formation: implications from atmospheric measurements for
763 nucleation and early growth mechanisms, Atmos. Chem. Phys., 6, 4079–4091, 2006.
764 Sipila, M., Berndt, T., Petaja, T., Brus, D., Vanhanen, J., Stratmann, F., Patokoski, J., Mauldin
765 III, R. L., Hyvarinen, A.-P., Lihavainen, H., and Kulmala, M.: Role of sulfuric acid in
766 atmospheric nucleation, Science, 327, 1243–1246, 2010.
767 Smith, J. N., Barsanti, K. C., Friedli, H. R., Ehn, M., Kulmala, M., Collins, D. R., Scheckman, J.
768 H., Williams, B. J., and Mc-Murry, P. H.: Observations of aminium salts in atmospheric
769 nanoparticles and possible climatic implications, P. Natl. Acad. Sci. USA, 107, 6634–6639,
770 2010.
771 Spracklen, D. V., Carslaw, K. S., Merikanto, J., Mann, G. W., Reddington, C. L., Pickering, S.,
772 Ogren, J. A., Andrews, E., Baltensperger, U., Weingartner, E., Boy, M., Kulmala, M.,
773 Laakso, L., Lihavainen, H., Kivekas, N., Komppula, M., Mihalopoulos, N., Kouvarakis, G.,
774 Jennings, S. G., O'Dowd, C., Birmili, W., Wiedensohler, A.,Weller, R., Gras, J., Laj, P.,
775 Sellegri, K., Bonn, B., Krejci, R., Laaksonen, A., Hamed, A., Minikin, A., Harrison, R. M.,
776 Talbot, R., and Sun, J.: Explaining global surface aerosol number concentrations in terms of
777 primary emissions and particle formation, Atmos. Chem. Phys., 10, 4775–4793, 2010.
778 Stanier, C. O., Pathak, R. K., and Pandis, S. N.: Measurements of the volatility of aerosols from
779 α-pinene ozonolysis, Environ. Sci. Technol., 41, 2756–2763, 2007.
780 Twomey, S.: Pollution and the planetary albedo, Atmos. Environ., 8, 1251–1256, 1974.
781 Twomey, S.: The Influence of pollution on the shortwave albedo of clouds, J. Atmos. Sci., 34,
782 1149–1152, 1977.
783 Twomey, S.: Aerosols, clouds, and radiation, Atmos. Environ., 25A, 2435–2442, 1991.
784 Tzivion, S., Feingold, G., and Levin, Z.: An efficient numerical solution to the stochastic
785 collection equation, J. Atmos. Sci., 44, 3139–3149, 1987.
786 Tzivion, S., Feingold, G., and Levin, Z.: The evolution of raindrop spectra. Part II: collisional
787 collection/breakup and evaporation in a rain shaft, Journal of the Atmospheric Sciences, 46,
788 3312–3327, 1989.
789 Tsimpidi, A. P., Karydis, V. A., Zavala, M., Lei, W., Molina, L., Ulbrich, I. M., Jimenez, J. L.,
790 and Pandis, S. N.: Evaluation of the volatility basis-set approach for the simulation of
791 organic aerosol formation in the Mexico City metropolitan area, Atmos. Chem. Phys., 10,
792 525-546, 2010.

Vehkamaki, H., Kulmala, M., Napari, I., Lehtinen, K. E. J., Timmreck, C., Noppel, M., and Laaksonen, A.: An improved parameterization for sulfuric acid-water nucleation rates for tropospheric and stratospheric conditions, J. Geophys. Res., 107, 4622–4632, 2002.

Wang, M. and Penner, J. E.: Aerosol indirect forcing in a global model with particle nucleation, Atmos. Chem. Phys., 9, 239–260, 2009.

Weber, R. J., Marti, J. J., McMurry, P. H., Eisele, F. L., Tanner, T. J., and Jefferson, A.: Measured atmospheric new particle formation rates: Implications for nucleation mechanisms, Chem. Eng. Commun., 151, 53–64, 1996.

Weber, R.J., et al.: A study of new particle formation and growth involving biogenic and trace gas species measured during ACE 1, J. Geophys. Res., 103, 16385–16396, 1998.

Weber, R.J., et al.: New particle formation in the remote troposphere: a comparison of observations at various sites, Geophys. Res. Lett., 26, 307–310, 1999.

Westervelt, D. M., Pierce, J. R., Riipinen, I., Trivitayanurak, W., Hamed, A., Kulmala, M., Laaksonen, A., Decesari, S., and Adams, P. J.: Formation and growth of nucleated particles into cloud condensation nuclei: model-measurement comparison, Atmos. Chem. Phys., 13, 7645–7663, 2013.

Westervelt, D. M., Pierce, J. R., and Adams, P. J.: Analysis of feedbacks between nucleation rate, survival probability and cloud condensation nuclei formation, Atmos. Chem. Phys., 14, 5577-5597, 2014.

Yli-Juuti, T., Nieminen, T., Hirsikko, A., Aalto, P. P., Asmi, E., Horrak, U., Manninen, H. E., Patokoski, J., Dal Maso, M., Petaja, T., Rinne, J., Kulmala, M., and Riipinen, I.: Growth rates of nucleation mode particles in Hyytiala during 2003– 2009: variation with particle size, season, data analysis method and ambient conditions, Atmos. Chem. Phys., 11, 12865–12886, 2011.

Yu, F.: Effect of ammonia on new particle formation: A kinetic H_2SO_4-H_2O-NH_3 nucleation model constrained by laboratory measurements, J. Geophys. Res., 111, doi:10.1029/2005JD005968, 2006a.

Yu, F.: From molecular clusters to nanoparticles: second-generation ion-mediated nucleation model, Atmos. Chem. Phys., 6, 5193–5211, 2006b.

822 Yu, F. and Luo, G.: Simulation of particle size distribution with a global aerosol model:
823 contribution of nucleation to aerosol and CCN number concentrations, Atmos. Chem. Phys.,
824 9, 7691–7710, 2009.
825 Yu, F.: A secondary organic aerosol formation model considering successive oxidation aging and
826 kinetic condensation of organic compounds: global scale implications, Atmos. Chem. Phys.,
827 11, 1083–1099, 2011.
828 Zhang, K.M., and Wexler, A.S.: A hypothesis for condensation of fresh atmospheric nuclei,
829 Journal of Geophysical Research, 107, doi:10.1029/2002JD002180, 2002.
830 Zhang, R.I., et al.: Atmospheric new particle formation enhanced by organic acids, Science, 304,
831 1487–1490, 2004.
832 Zhang, Y., McMurry, P. H., Yu, F., and Jacobson, M. Z.: A comparative study of nucleation
833 parameterizations: 1. Examination and evaluation of the formulations, J. Geophys. Res.,
834 115, doi:10.1029/2010JD014150, 2010.
835 Zhao, J., Smith, J. N., Eisele, F. L., Chen, M., Kuang, C., and McMurry, P. H.: Observation of
836 neutral sulfuric acid-amine containing clusters in laboratory and ambient measurements,
837 Atmos. Chem. Phys., 11, 10823–10836, 2011.

838

839

840 **Table 1.** Main inputs of DMANx simulations.

Inputs	**Hyytiala (Finland)**	**Finokalia (Greece)**
Temperature	Measurements	Model PMCAMx
RH	Measurements	Model PMCAMx
O_3	Measurements	Model PMCAMx
OH	Model PMCAMx	Model PMCAMx
SO_2	Measurements	Measurements
NH_3	Measurements (PTR-MS)	Measurements
TERP	Measurements (PTR-MS)	Model PMCAMx
ISOP	Measurements (PTR-MS)	Model PMCAMx
ARO1	Measurements (PTR-MS)	Model PMCAMx
ARO2	Model PMCAMx	Model PMCAMx
ALK4	Model PMCAMx	Model PMCAMx
ALK5	Model PMCAMx	Model PMCAMx
Initial number distributions	Measurements (DMPS)	Measurements (SMPS)

841

842

843

844

845

846

847

848

849

850

851

852

853

854

855

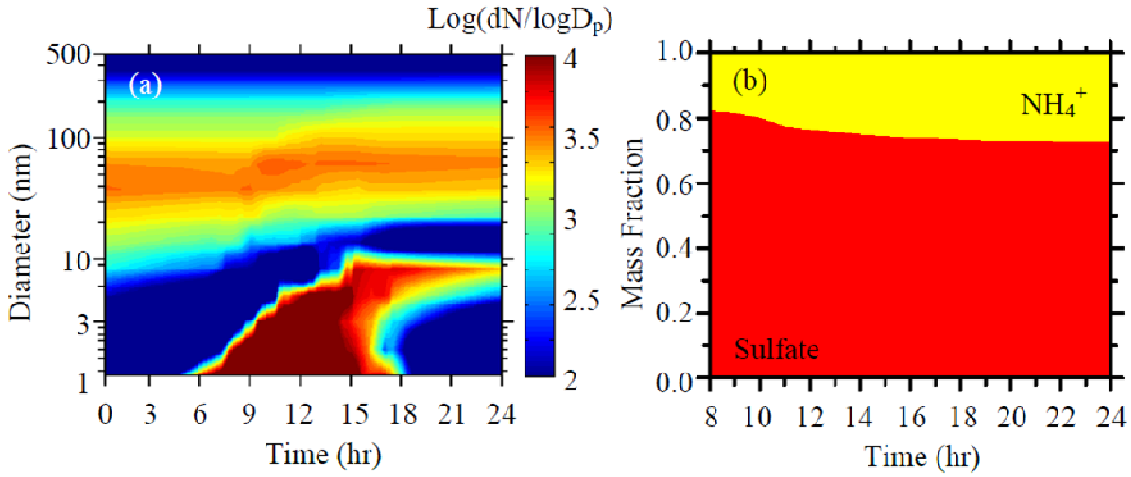

FIGURE 1: a) Predicted aerosol dry size distribution for a typical spring nucleation event at Hyytiala without condensation of organics. Particle number concentration is plotted against local time of day (x-axis) and particle diameter (y-axis). b) Predicted composition of new particles.

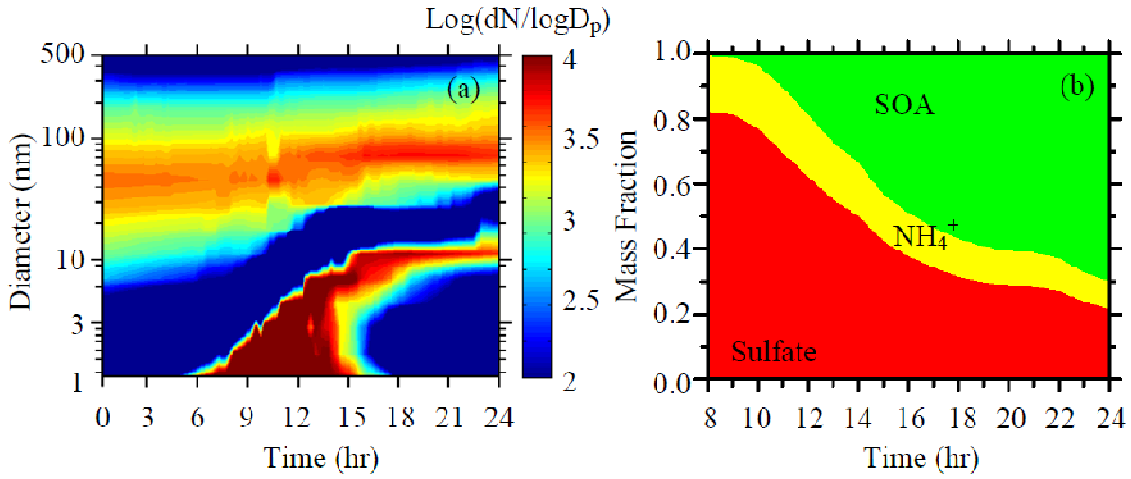

FIGURE 2: Simulation with surface tension σ=0.025 N m^{-1} at Hyytiala: a) predicted particle size distribution with number concentration plotted against time of day (x-axis) and particle diameter (y-axis) and b) the composition of new particles.

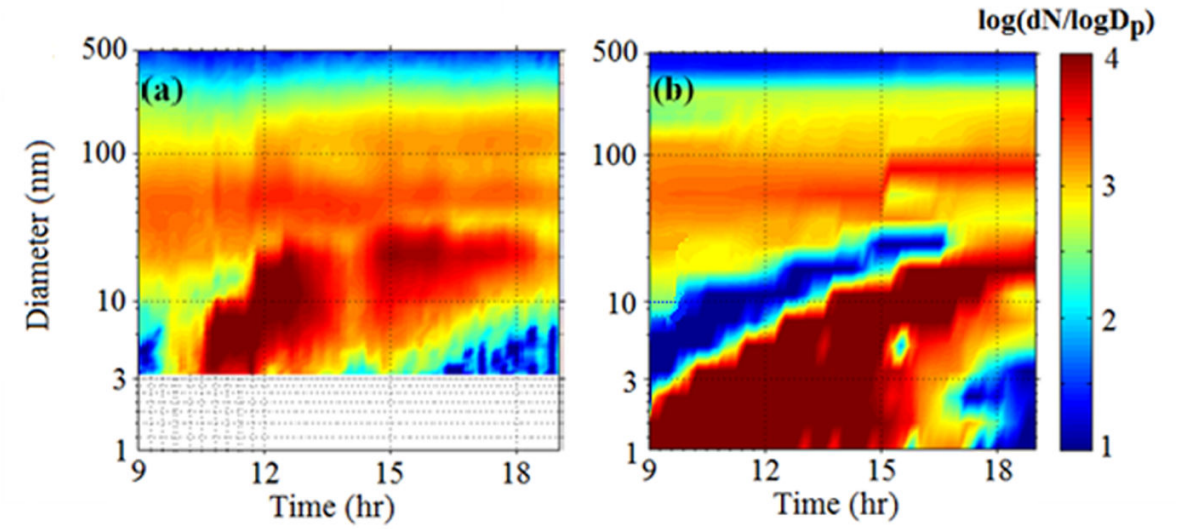

FIGURE 3: Comparison of (a) measured on 10 April 2007 and (b) predicted (with aging of bSOA precursors and σ=0.025 N m^{-1}) dry size distribution as a function of local time at Hyytiala for a typical nucleation event day.

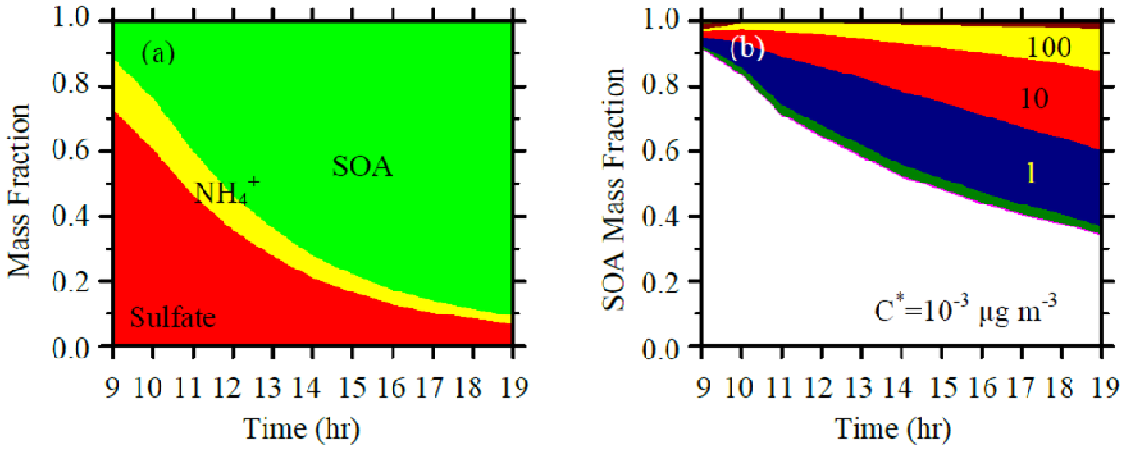

FIGURE 4: a) Mass fraction of fresh particles and b) mass fraction of SOA for the different volatility bins as a function of local time at Hyytiala. Simulation includes bSOA aging and σ=0.025 N m^{-1}.

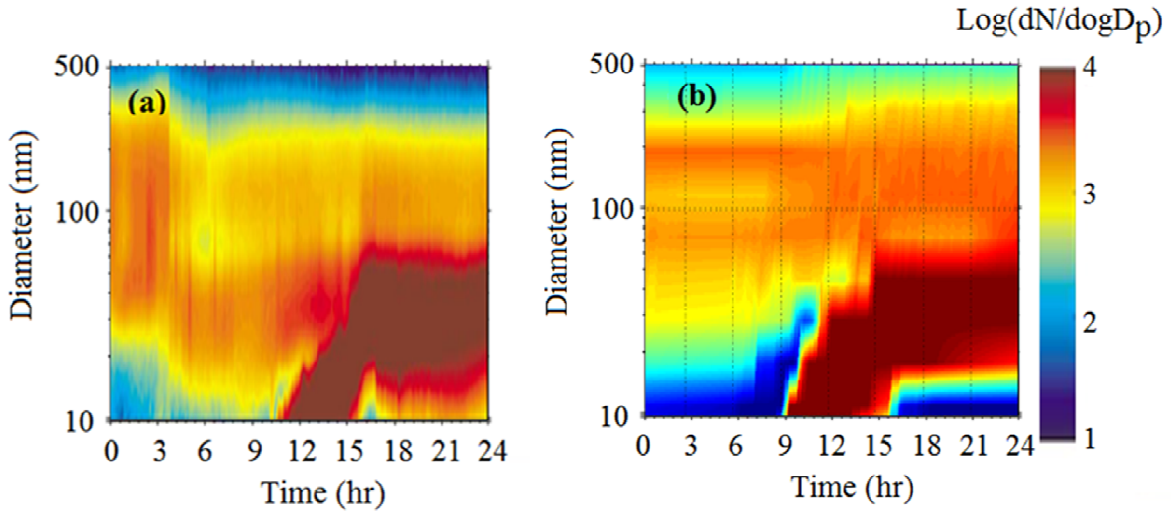

946

947 **FIGURE 5:** Comparison of (a) measured on 19 March 2009 (Pikridas et al., 2012) and (b)
948 predicted dry size aerosol distribution (with bSOA aging and σ=0.025 N m^{-1}) as a function of
949 time at Finokalia.

950

951

952

953

954

955

956

957

958

959

960

961

962

963

964

965

966

967

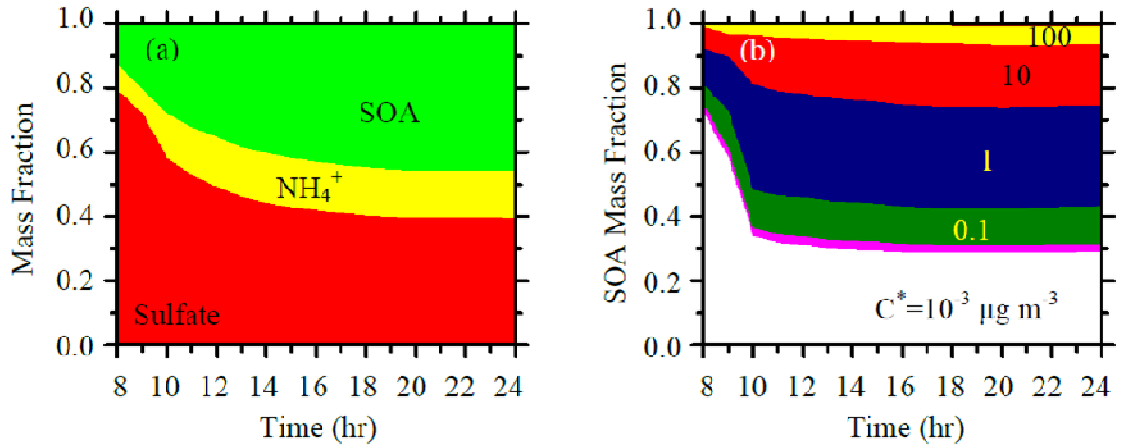

FIGURE 6: a) Mass fraction of fresh particles and b) mass fraction of SOA for the different volatility bins as a function of local time at Finokalia. Simulation includes bSOA aging and σ=0.025 N m^{-1}.

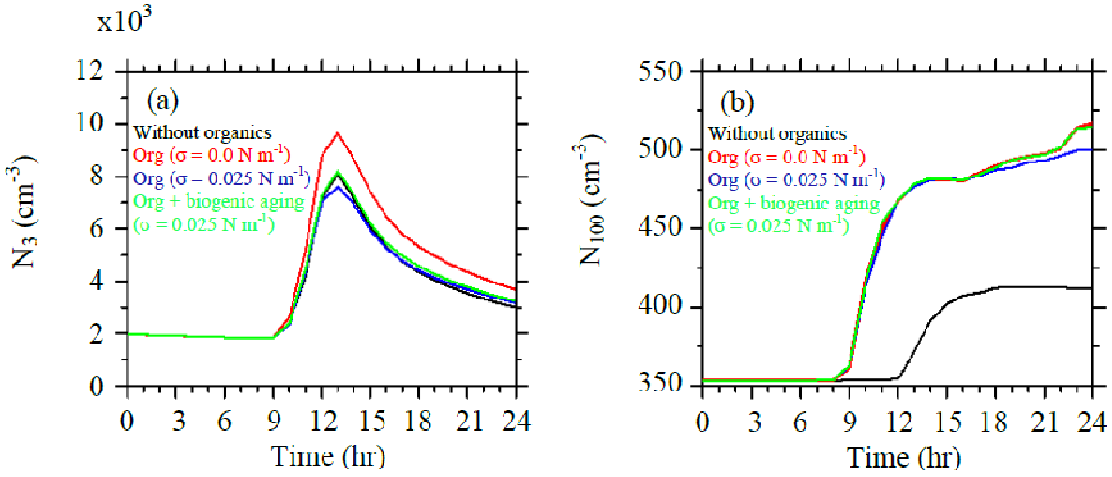

991

992 **FIGURE 7:** Predicted concentrations of a) N_3 and b) N_{100} at Hyytiala for the four simulated
993 cases. Black line represents no condensation of organics, red is with condensation of organics
994 with σ = 0.0 N m^{-1}, blue is with condensation of organics with σ = 0.025 N m^{-1} and green is
995 condensation of organics with aging reactions of bSOA precursors and σ=0.025 N m^{-1}.

996

997